

# Application of Plasma Technology in Fischer-Tropsch Catalysis for the Production of Synthetic Fuels



James Aluha, François Gitzhofer and Nicolas Abatzoglou\*

Department of Chemical and Biotechnological Engineering, Université de Sherbrooke, Canada

Submission: April 23, 2018; Published: May 08, 2018

\*Corresponding author: Nicolas Abatzoglou, Department of Chemical and Biotechnological Engineering, Université de Sherbrooke, Québec, J1K 2R1, Canada, Tel: +1 (819) 821-7904; Email: nicolas.abatzoglou@usherbrooke.ca

## Abstract

A short review of our results is presented on the use of high temperature plasma technology in producing catalysts for application in Fischer-Tropsch synthesis (FTS). Nanometric carbon-supported catalysts based primarily on Co and Fe with various metal formulations were synthesized using an induction suspension plasma-spray (SPS) system. The active catalytic species of the metals and the C-matrix support composing both graphitic (G) and amorphous (D; disordered) carbon were all simultaneously generated in situ within the plasma. The Co/C catalyst was the most active when tested for FTS with high selectivity towards the longer hydrocarbon chains. At 220 °C, 2MPa pressure; gas hourly specific velocity of over 3,600cm<sup>3</sup>.h<sup>-1</sup>.g<sup>-1</sup> of catalyst, it indicated ~40% CO conversion with the following selectivity expressed as % in the products: 30% gasoline (C<sub>5</sub>-C<sub>12</sub>), 45% diesel (C<sub>13</sub>-C<sub>20</sub>), and 21% waxes (C<sub>21+</sub>), with less than 4% CH<sub>4</sub> and trace amounts of CO<sub>2</sub>. Other catalysts tested include Fe/C, bimetallic Co-Fe/C formulations and those promoted with Ni, Mo, and Au-Ni. It has been shown that particle size influences FTS when using plasma-synthesized catalysts: thus, particles in the mean size range of 9-11nm were more selective towards the diesel fraction and waxes, while larger particles of mean size of 14-21nm produced more gasoline. Since SPS technology is a relatively new approach in catalyst synthesis, being a one-step process potentially offers an overall higher efficiency and new prospects for the commercial production of synthetic fuels through FTS.

**Keywords:** Fischer-Tropsch; Catalysts; Plasma-synthesis; Carbon support

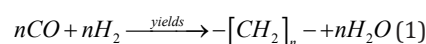
**Abbreviations:** OAC: Alternating Current; ASF: Anderson-Schulz-Flory Product Distribution; BET: Brunner-Emmett-Teller (Surface Area Analysis); BTL: Biomass-To-Liquid; C<sub>4</sub>-C<sub>12</sub>: Gasoline Fraction; C<sub>13</sub>-C<sub>20</sub>: Diesel Fraction; C<sub>21+</sub>: High Molecular Hydrocarbons, Such As Waxes STR: Continuously-Stirred Tank Reactor; CTL: Coal-To-Liquid; D: Disordered or Amorphous Carbon; DBD: Dielectric Barrier Discharge Plasma; EDX: Energy Dispersive X-Ray Spectroscopy; FCC: Face-Centered Cubic Structure; FTS: Fischer-Tropsch Synthesis; G: Graphitic Carbon; GC: Gas Chromatography; GHSV: Gas Hourly Space Velocity; GTL: Gas-To-Liquid; HT-FTS: High Temperature Fischer-Tropsch Synthesis; HCP: Hexagonal Closed Packing; LT-FTS: Low Temperature Fischer-Tropsch Synthesis; NTP: Non-Thermal Plasma Reactor; P: Pressure (Pa); RF: Radio Frequency; RQA: Rietveld Quantitative Analysis; SEM: Scanning Electron Microscopy; SPS: Suspension Plasma-Spray Technology; T: Temperature(K); TEM: Transmission Electron Microscopy; TOS: Time-On-Stream; 3φ-CSTR: Three-Phase Continuously-Stirred Tank Slurry Reactor; XANES: X-ray Absorption Near-Edge Structure; XPS: X-ray Photoelectron Spectroscopy; XRD: X-ray Diffraction

## Introduction

Fischer-Tropsch Synthesis (FTS) was discovered in the 1920's by Franz Fischer and Hans Tropsch, and since then, FTS has been studied extensively [1], with four metals, namely Co, Fe, Ni and Ru exhibiting great potential for catalytic application. However, only Co and Fe are commercially exploited today [2] to produce synthetic automobile fuels such as gasoline, diesel and many other valuable hydrocarbon products [3]. Working at the lowest reaction temperature of only 150 °C, Ru catalyst is the most active FTS catalyst, yielding products of high molecular weight, but it is expensive [4], while Ni forms nickel carbonyls at high pressure and generates mainly CH<sub>4</sub> at higher temperatures [5].

Though very complex due to the occurrence of a high number of desired and undesired side reactions, FTS can be simply viewed as a process that converts syngas (a mixture of

H<sub>2</sub> and CO in a specified ratio) to form polymeric chains of liquid hydrocarbons with a widespread distribution of products as represented by Equation (1):



FTS works in two modes. The high-temperature process (HT-FTS) operates on Fe-based catalysts between 300-350 °C and produces mainly gasoline and linear low molecular-mass olefins, while the low-temperature process (LT-FTS) operates between 200- 240 °C using Co catalysts, which produce high molecular-mass hydrocarbons and linear waxes [1]. Product separation into various fractions is accomplished through distillation columns, and since some product overlaps exist in the components, in this discussion the fractions are classified as follows: gasoline (C<sub>5</sub>-C<sub>12</sub>), diesel (C<sub>13</sub>-C<sub>20</sub>) and waxes (C<sub>21+</sub>).

Numerous concerns have been expressed involving global warming in particular, and due to increased greenhouse gases in the atmosphere [6], it is generally thought that future production of cleaner fuels will benefit from the FTS path. Increasing regulatory measures through stringent legislation, as well as the push for sulphur-free diesel are seen as the main drivers, as our society endeavours to replace a part of the fossil fuels with biofuels [7]. In addition, application of bio-syngas in FTS is attractive because biomass is the cheapest and most abundant renewable source of hydrocarbons in nature [8], and for commercial production of gasoline or diesel, the lowest cost path would be the most favourable. FTS being a versatile process by design, it has capacity to adapt to diverse feed stocks such as natural gas, coal or biomass, from which their respective names are attributed: (a) gas-to-liquid (GTL), (b) coal-to-liquid (CTL), and (c) biomass-to-liquid (BTL) processes [9]. The hydrocarbons thus produced are comparable to the conventional liquid fuels derived from crude oil when refined without containing sulphur and aromatics.

Application of plasma techniques for catalyst synthesis was initiated in the 1980s based on plasma spraying or glow discharge plasma [3]. For example, in some of the earliest works where plasma-spraying was used, five catalysts (100%Fe, 75%Fe-25%Co, 50%Fe-50%Co, 25%Fe-75%Co, and 100%Co on w/w percent basis) were synthesized and they showed the presence of various phases on the catalyst surface, namely, Fe and Co oxides and cemented particles of  $\text{CoO-Fe}_2\text{O}_3$  [10]. It is doubtful that such catalysts would be applicable in FTS directly without further treatment because sufficient evidence has indicated that Fe catalyzed FTS reaction mechanism depends on the presence of Fe carbides [11]. Currently in industry, the Fe carbides are generated mainly by carburizing the Fe oxides with CO [12]. By the application of induction suspension plasma-spray (SPS) technology one can generate these Fe carbides directly from the metal and carbon support, where only the excess C-matrix is gasified in order to expose the active sites to the FTS feed gas [13].

Some other authors have applied plasma pre-treatment through glow discharge to decompose Co-nitrate at much lower temperatures than conventional calcination of the Co-based FTS catalysts in order to produce smaller super paramagnetic Co metal nanoparticles of size less than 7 nm [14]. Since the active species for Co-based catalysts in FTS is in metallic form [15], this catalyst having shown a 26% CO conversion was found to compete favourably with the conventional Pt-promoted catalyst yielding 19- 24% CO conversion under similar reaction conditions [14]. In addition, it was observed that higher Co dispersion accompanied by ease of reducibility leads to higher catalytic activity of the plasma-treated FTS catalysts. In yet another study, plasma pre-treatment was seen to significantly enhance the Co dispersion in silica- supported catalysts and the Co-particle size was perceived to be a function of glow discharge

plasma intensity, while plasma pretreatment of the Ru-promoted catalyst exhibited an enhanced FTS activity [16].

Equally, there is growing interest in the application of non-thermal plasma (NTP) reactors for FTS, which may provide viable alternatives to conventional processes that may operate with or without a catalyst. In one study,  $\text{C}_1\text{-C}_3$  hydrocarbons were synthesized at high pressure ( $P > 1$  MPa) without a catalyst [17]. It has been shown that combining plasma with catalysts can produce new reactive species, plasma photon emissions or thermal hotspots that can initiate catalytic reactions [18]. NPT technology requires minimal space and its low cost maintenance motivates for its application. Reaction rapidity (ranging from nanoseconds to minutes) promoted by highly active NTP species at ambient temperature is one among the many advantages of the non-thermal arc discharge process [17].

The dielectric barrier discharge (DBD) plasma has been observed to promote FTS over a Cu/Co-based catalyst at low temperatures and ambient pressure. It has been shown that plasma strongly suppresses  $\text{CH}_4$  production, and, as opposed to the conventional FTS process, CO conversion in the DBD-promoted FTS was much higher at low operating pressure than at higher pressure, indicating a new FTS reaction path [19]. Several other studies reveal that plasma treatment offers many positive effects leading to higher CO conversion, lower temperature activity and better suppression of coke deposition, besides better metal dispersion, smaller  $\text{CO}_3\text{O}_4$  cluster size, and more uniform Co distribution [20]. These results show that not only is plasma able to improve the structural properties of the catalysts, but also to enhance the reaction activity and products yield.

Current advancement in the production of synthetic fuels involve the application of induction SPS technology to produce nanometric catalysts that inherently consist of active catalytic species for FTS, that is, Fe carbides and metallic Co [13]. Therefore, the primary objective of this study was to compare different features of the FTS process, such as sample preparation methods, characterization of the catalytic properties of the materials and measurement of the performance of the catalysts. It has been shown that all catalysts produced through SPS technology (Co-only, Fe-only, Co-Fe bimetallics and those promoted with Au, Ni and Mo) consist a myriad of species and phases ranging from metallic to carbidic species. Although the relative activity of these phases is not yet quantified, all synthesized catalysts are proven to be highly active for FTS as determined from their catalytic activity and selectivity. The above described materials have been found to be nanometric and non-porous; these features lead to surface reaction kinetics, operating away from mass-diffusion controlled FTS regimes. One of the positive impacts is that, at relatively  $\text{H}_2$ -poor feeds (low molar  $\text{H}_2/\text{CO}$ ), the  $\text{CH}_4$  selectivity is significantly lower than with classical FTS catalysts [21].

With various aspects of the FTS process having been considered as shown in Figure 1, only a few areas have been examined so far due to the breadth of the subject, to which this research work has contributed new knowledge. Therefore, we begin by underscoring the major contribution SPS technology has played in the success of this work by efficiently producing highly active FTS catalysts [22]. It has been observed that the plasma method provides better catalyst composition reproducibility, which is achieved within shortened preparation time when

compared to other methods such as impregnation [23], and precipitation [24]. This is mainly attributed to the fact that it is a single-step approach, producing robust catalysts whose metal components do not sinter [25]. Other authors assert that plasma methods produce materials of superior catalytic performance [26], evenly distributed active species that are characterized by longer catalyst lifetime and overall lower energy requirements [27,28].

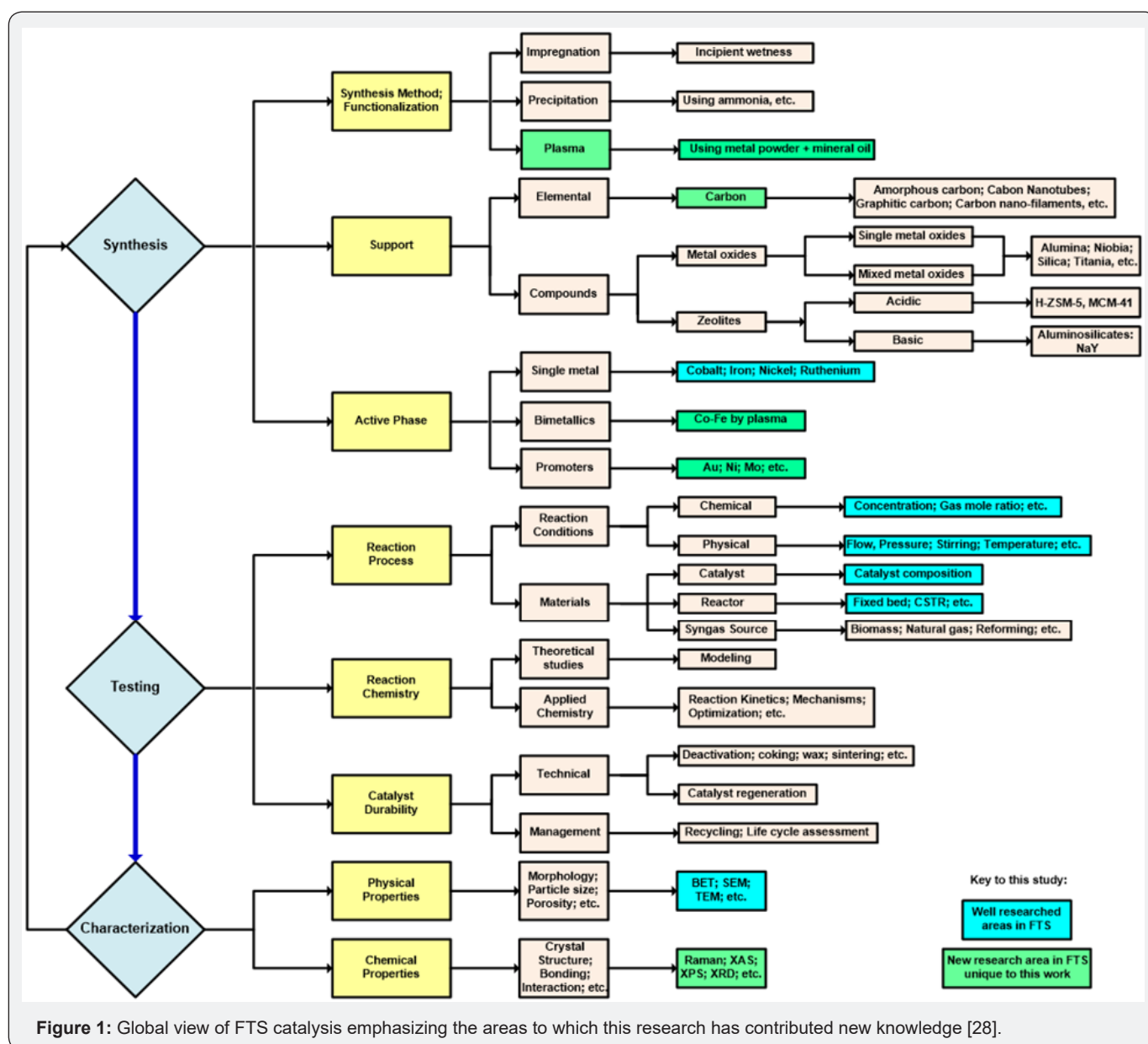


Figure 1: Global view of FTS catalysis emphasizing the areas to which this research has contributed new knowledge [28].

### Experimental Methods

Using the PL-50 plasma torch supplied by Tekna Inc., the induction suspension plasma-spray (SPS) system operates at 3.2MHz alongside other system parameters, which are fully described in earlier works [29]. In order to enhance the production of ionic species in the plasma, radio frequency (RF)

alternating currents (AC) generate an oscillating magnetic field in a coil set around the plasma plume, which couples to the partially ionized gas flowing through the coil. The reactor set-up is provided and fully described elsewhere [22]. A homogeneous mixture of 60g of the metal (particle size range 1-10µm) in 300cm<sup>3</sup> of mineral oil was introduced directly into the plasma using an atomization probe at a flow rate of 8.2cm<sup>3</sup>.min<sup>-1</sup> while

maintaining the triode plate power at 29kW [25]. After catalyst synthesis, the powder materials were collected from the sides of the reactor vessels and analyzed.

The FTS reaction tests were performed in a high-pressure, Autoclave Engineers (Erie, PA, U.S.A) stainless- steel vessel. This was isothermally operated as a three-phase continuous-stirred tank slurry reactor (3- $\phi$ - CSTR) at 220-260 °C temperature range and 2MPa pressure. About 5g of the catalyst was used with a gas feed stock of molar H<sub>2</sub>: CO=2, flowing at 300cm<sup>3</sup>.min<sup>-1</sup> or gas hourly space velocity (GHSV) of about 3,600cm<sup>3</sup>.h<sup>-1</sup>.g<sup>-1</sup> of catalyst. Prior to the FTS reaction the catalysts were pre-treated in situ (because the materials are pyrophoric), at 400 °C for 24h under reducing conditions of pure H<sub>2</sub> or CO flowing at 250cm<sup>3</sup>.min<sup>-1</sup>. In order to ensure that the FTS reaction operated outside diffusion limitations,

- a. a nanometric catalyst was envisaged, and
- b. The system was agitated with a stirring speed of over 2,000rpm. As a confirmation, an experiment doubling the mass of the catalyst to 10g was performed, with an expectation that the CO conversion would also double. Both catalyst activity and selectivity were determined by GC analyses [30].

These catalysts were tested for FTS and found to be characteristically active:

- a. Two single metal (Co/C and Fe/C) benchmarked against the commercial hematite Fe-NanoCat® [30], with the minimum testing time required to define a catalyst's  $\alpha$ -value determined using the Co/C sample [31].
- b. Three bimetallic formulations (30%Co-70%Fe/C, 50%Co-50%Fe/C and 80%Co-20%Fe/C) tested after reduction in H<sub>2</sub> or CO [32].
- c. Two ternary formulations simulating promotion of the 80%Co-20%Fe/C sample (10%Mo-70%Co-20%Fe/C and 10%Ni-70%Co-20%Fe/C) and in this discourse are abbreviated as Mo-Co- Fe/C, Ni-Co-Fe/C respectively [33].
- d. The 5%Ni-70%Co-25%Fe/C, which was later promoted with ~5% Au doping, (abbreviated as Au- Ni-Co-Fe/C).

All the single metal, bimetallic and ternary metal formulations have been fully characterized for their specific surface areas by the Brunauer-Emmett-Teller (BET) method, metal particle dispersion and analysis for particle size distribution has been conducted using transmission electron microscopy (TEM) [22]. Scanning electron microscopy (SEM), coupled with the energy dispersive X-ray spectroscopy (EDX) was used to confirm metal particle dispersion in the C-matrix by EDX-mapping [22]. Phase identification and quantification has been attempted using powder X-ray diffraction (p-XRD) analysis in conjunction with Rietveld quantitative analysis (RQA) [30], with catalyst evaluation results by X-ray photoelectron spectroscopy (XPS) and X-ray absorption near-edge structure (XANES) confirming

some of the XRD data [25].

### Results and Discussion

Plasma applications are currently receiving a lot of attention because, when viewed in the broader context of global technology trends, they continue to find new industrial applications in materials processing including the development of commercial catalysts [34]. In this work, we show that FTS catalysts produced through SPS technology were both nanometric and non-porous. Since nanometric catalysts are imperative in overcoming mass transfer limitations in the FTS process, the aim was to produce both the active phase (containing the metallic moieties) and the carbon support of different forms (the disordered, D and the graphitic, G) in the nanometric range.

The use of plasma is therefore an attempt to produce high quality catalysts by means of a less complex method. After method optimization with the Fe-only FTS catalytic formulation, the same recipe was applied with the same success for all other catalyst formulations. This preserves the distinct qualities of the materials despite variation in metal composition. In addition, having the catalysts supported on nanometric carbon, no adverse effects have been observed in the catalyst performance so far, although deactivation by C deposition is rampant in most FTS catalysts, which means that not all forms of carbon lead to deactivation [35]. Therefore, catalyst synthesis through plasma presents a unique way of producing high quality FTS catalysts, with potential for commercialization.

### Catalyst characterization

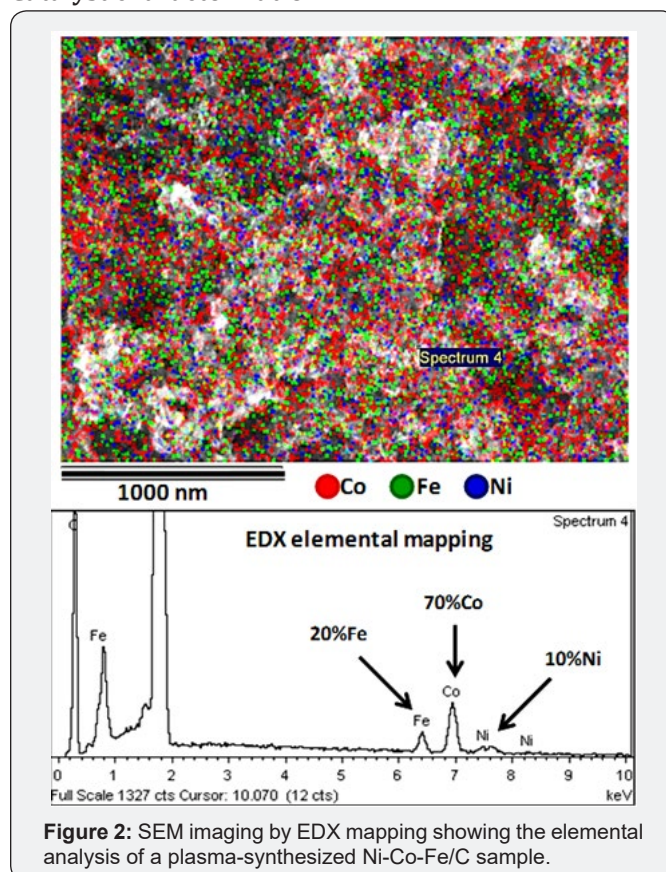
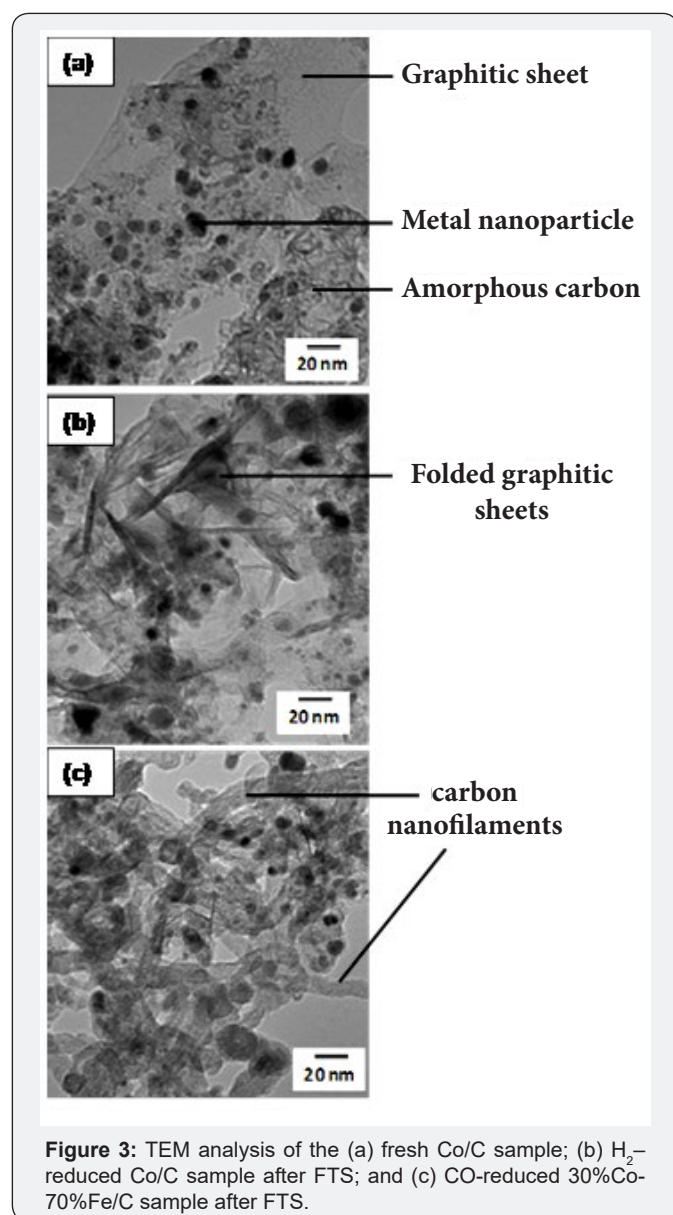


**Figure 2:** SEM imaging by EDX mapping showing the elemental analysis of a plasma-synthesized Ni-Co-Fe/C sample.

**BET surface area analysis:** The plasma-synthesized materials were analyzed and found to have BET specific surface area in the range of 35-93m<sup>2</sup>.g<sup>-1</sup>, with the single-metal catalysts having the lowest surface areas [22]. The catalysts were also shown to be non-porous from their characteristic overlaid adsorption and desorption isotherms, which is advantageous because it enables the FTS reaction to operate away from mass transfer limitations.

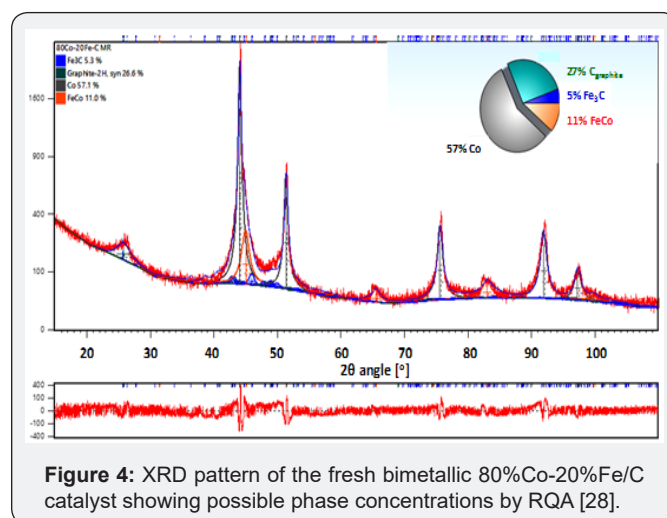
**Scanning electron microscopy:** SEM imaging portrayed high metal dispersion in the C-matrix, attesting to the high quality of the materials synthesized by plasma. Figure 2 indicates that there was no preferential metal deposition or metal segregation because of the apparent uniform distribution of the all the three metals across the C-matrix.



**Transmission electron microscopy:** TEM analysis indicated consistent particle-size distribution and that both the fresh and used single-metal Co/C and Fe/C catalysts had a mean particle of ~9nm [30]. The 80%Co-20%Fe/C and 30%Co-70%Fe/C

bimetallic samples had mean of ~11nm, but only the 50%Co-50%Fe/C sample was unique with a much higher mean of ~14nm, possibly because it contained more CoFe nano-alloys [32]. Figure 3a & 3b indicates that there was very little difference in the catalyst's morphology after conducting the FTS reaction except for the augmented creasing of the graphitic sheets, although there was very little evidence to show any major change in the metal particle size during FTS reaction [30], particularly when H<sub>2</sub> was used for catalyst activation. However, with CO reduction, the C-matrix in Fe-containing samples converted into carbon nanofilaments and this is exemplified in Figure 3c [32].

**X-ray diffraction analysis:** XRD analysis in conjunction with RQA gave some indication of the phases present in the samples although the materials being amorphous made absolute quantification difficult. As seen in Figure 4, XRD identified easily both the metallic species and graphitic-C. However, confirmation of carbide species by other techniques such as XPS was difficult though they were detected by XRD. For example, in the single-metal samples, the presence of Fecarbides (Fe<sub>2</sub>C, Fe<sub>3</sub>C, Fe<sub>5</sub>C<sub>2</sub>) was recognized in the Fe/C and possibility of Cocarbides (Co<sub>2</sub>C, Co<sub>3</sub>C) was high in the Co/C [30], but XPS could not detect these carbides [25]. In addition, the same carbide species were perceived in the bimetallic Co-Fe/C formulations, but in small quantities alongside nano-alloys such as CoFe, Co<sub>3</sub>Fe<sub>7</sub> and Co<sub>7</sub>Fe<sub>3</sub> [32].



### Catalyst activity testing

Initial FTS catalyst activity was recorded with time-on-stream (TOS) for over 25h by sweeping over a range of temperatures, as shown in Figure 5. Using the single metal Co/C catalyst, the average activity was shown to be about 40% CO conversion at 220 °C, 50% CO conversion at 230 °C, over 65% CO conversion at 240 °C, and total CO conversion at 260 °C. Since the catalysts proved to be highly active, rapid consumption of the feedstock gases produced significant pressure drops and temperature spikes that led to significant fluctuations in readings. Figure 6 was a reproducibility test, where four different samples of the same (Co/C) catalyst were reduced and tested separately for

FTS, and all the data points were averaged, with the overall activity found to be about 41% CO conversion at 220 °C, 2 MPa pressure and GHSV of 3,600cm<sup>3</sup>.h<sup>-1</sup>.g<sup>-1</sup> of catalyst. The scatter of the data points indicated a standard deviation, ( $\sigma$ ) of 3%.

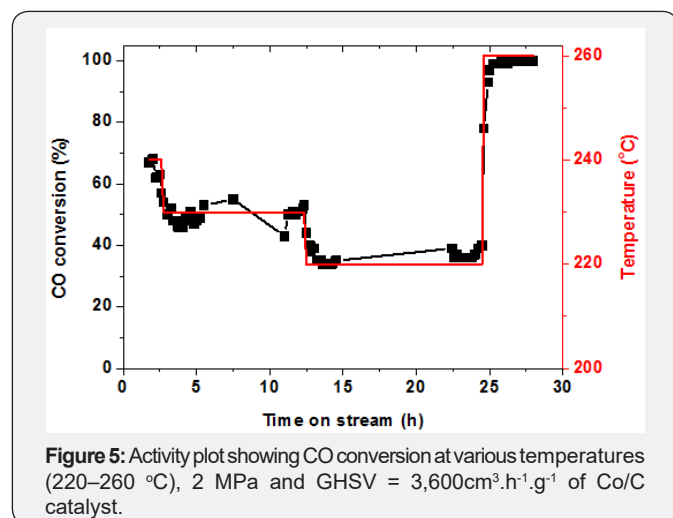


**Figure 5:** Activity plot showing CO conversion at various temperatures (220–260 °C), 2 MPa and GHSV = 3,600cm<sup>3</sup>.h<sup>-1</sup>.g<sup>-1</sup> of Co/C catalyst.

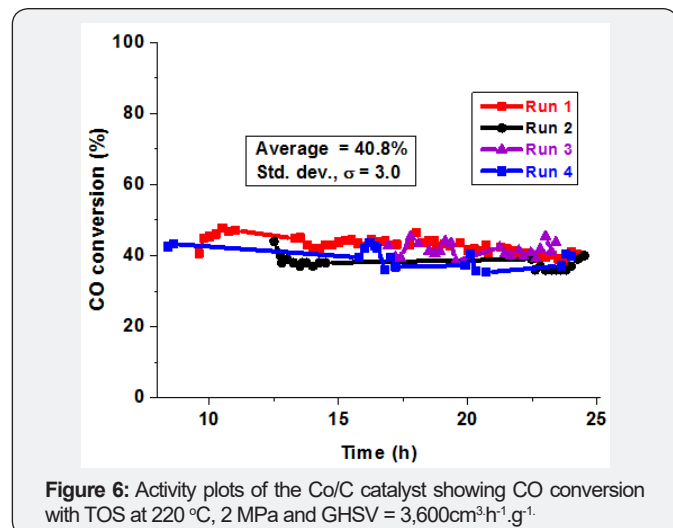


**Figure 6:** Activity plots of the Co/C catalyst showing CO conversion with TOS at 220 °C, 2 MPa and GHSV = 3,600cm<sup>3</sup>.h<sup>-1</sup>.g<sup>-1</sup>.

In order to confirm that the reaction was operated outside diffusion limitations, doubling the catalyst mass to 10g (GHSV of 1,800cm<sup>3</sup>.h<sup>-1</sup>.g<sup>-1</sup> of catalyst) increased its activity by almost double to 78% CO conversion. The main reason for operating away from diffusion-limited regimes is that FTS is a polymerization reaction and the inevitable formation of the heavier molecular weight and longer hydrocarbon chains with TOS eventually lead to catalyst deactivation due to clogging of the catalyst pores. This observation assists in determining the catalyst's lifespan and possibly the cause of its activity loss with TOS. In our case, catalyst activity seemed to be stable in the first 24h. The Co/C catalyst was observed to be the most active catalyst, followed by the Fe/C catalyst in comparison to the bimetallic Co-Fe/C formulations [32]. In addition, catalyst activation by H<sub>2</sub> reduction was perceived to produce more active materials than those activated by CO reduction, while Ni-addition to the bimetallic Co-Fe/C catalyst enhanced its activity from 42 to 50%

CO conversion [33], but Mo-addition slightly depressed catalyst activity to 38%.

It is advanced that during synthesis, plasma produced nano-alloy species (such as CoFe, Co<sub>3</sub>Fe<sub>7</sub> and Co<sub>7</sub>Fe<sub>3</sub>) in the bimetallic samples (as established from RQA and XRD analysis), which seem to be less available for FTS, thus leading to lower catalytic activity. This may be related to the inactive portion of the material being mixed with an active metal, resulting in some degree of dilution of the more active metal phase [36]. Although various studies demonstrate an inconsistent stability behaviour of bimetallic catalysts towards their activity, selectivity and deactivation [37], higher CO conversion was observed with increasing Fe content up to 0.5 wt% for CoFe supported on carbon nanotubes [38]. Alloying Co with Ni, for example, has been shown to be effective in enhancing the CO hydrogenation activity [39]. For the Fe-Co/SiO<sub>2</sub> systems, higher activity was observed in the Co-rich system [36], while the presence of small amounts of CoFe alloys was also related to an increased selectivity for alcohols [38]. However, the overall activity for the bimetallic systems, decreases with an increase in Fe content [36].

In Fe-catalyzed FTS, carbides are viewed to be the most active species because a process that replenishes them seems to enhance the reaction [40]. However, some controversy persists because one school of thought asserts that both magnetite and metallic Fe are active for FTS, while the carbides are inactive. Yet another school of thought advances that WGS reaction occurs on magnetite sites, while FTS takes place on the carbide sites [41]. Other authors claim that the non-stoichiometric Fe-oxide-carbide complex is the active phase [42]. Nevertheless, original findings from the use of SPS technology in catalyst synthesis demonstrated the benefit of plasma method in creating the Fe-carbides, which are thought to be indispensable in FTS [13]. Although the FTS reaction mechanism remains unclear, production of carbides partly guided the decision for catalyst choice, supported by C-material such as graphite [43]. Despite these differences in opinion, it is our view that these nano-alloys do not play a crucial role in FTS.

### Catalyst selectivity

From the initial studies carried out using the single-metal catalysts, it was shown that the plasma-synthesized Co/C catalyst was more selective towards the formation of longer-chain hydrocarbons, with massive waxes being displayed [30]. The kinetics of the FTS reaction involve the catalyst's alpha value ( $\alpha$ ), which denotes the probability for hydrocarbon-chain growth [44], and the prediction is expressed in the form of the Anderson-Schulz-Flory (ASF) distribution given by Equation (2) below [45].

$$\frac{M_n}{n} = (1 - \alpha)^2 \cdot \alpha^{(n-1)} \quad (2)$$

Where:  $M_n$  = mole fraction of a hydrocarbon with chain length  $n$

$n$  = number of total carbon atoms

$\alpha$  = probability of chain growth ( $\alpha < 1$ )

$(1 - \alpha)$  = probability of chain termination

The  $\alpha$ -value of the Co/C catalyst (for  $n > 10$ ), was found to be in the range of 0.8-0.9 depending on the feedstock composition, where the CO-rich feed gas mimicking a bio-syngas source registered a higher value [31] (Figure 7). On the other hand, the plasma-synthesized Fe/C catalyst formed less waxes, but showed an identical  $\alpha$ -value of over 0.8, which sharply contrasts with the commercial nano-hematite, Fe-NanoCat<sup>®</sup> that had an  $\alpha$ -value of 0.7 as expected. Normally, the  $\alpha$ -value for Co lies in the range of 0.7 – 0.8, while Fe operates between 0.5 – 0.7 [46].

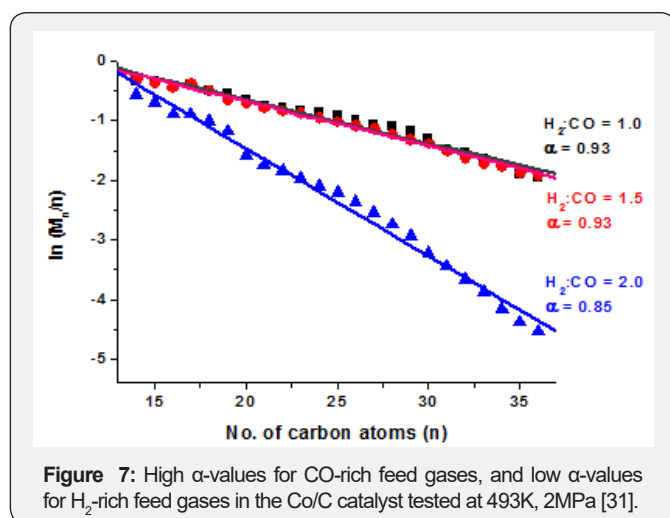
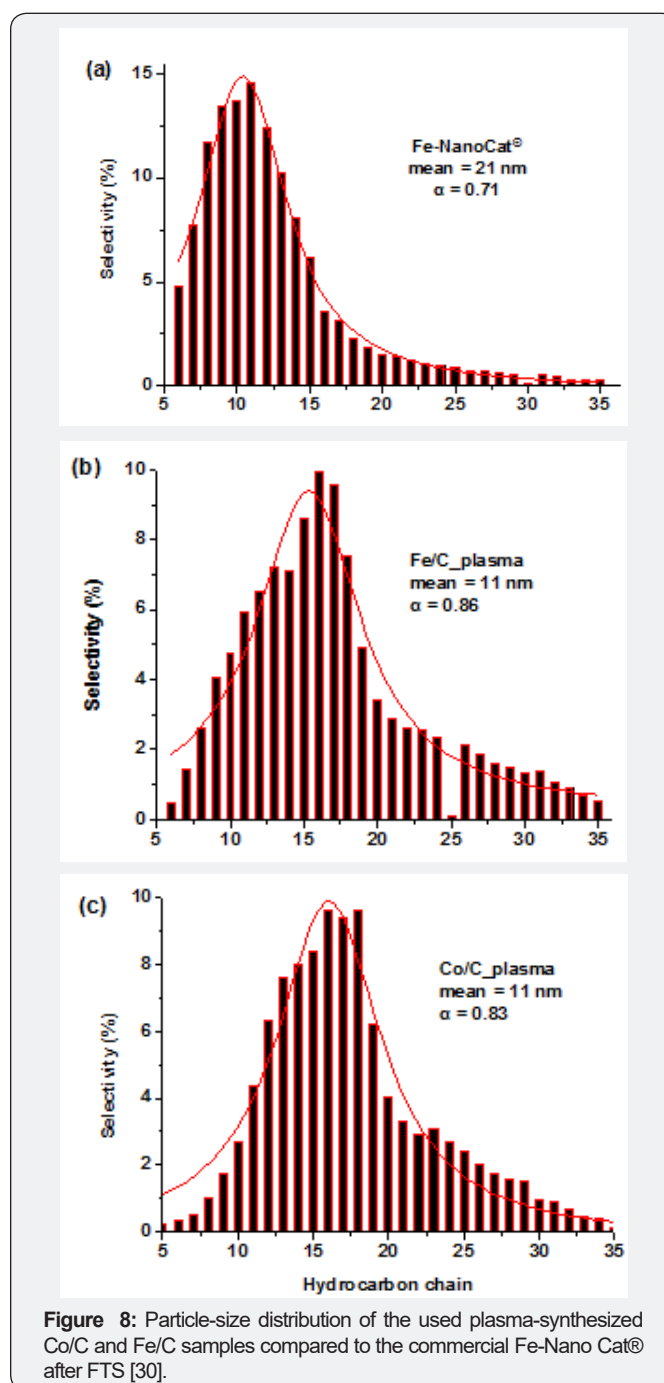


Figure 8 shows that by targeting for metal nanoparticles of mean size of approximately 10 nm in plasma-synthesized catalysts, the materials would produce more of the longer-chain hydrocarbons than gasoline fraction because the smaller the catalyst, the higher it's  $\alpha$ -value [47]. Usually, high  $\alpha$ -values at low temperature favour production of diesel and high molecular-mass hydrocarbons (e.g. waxes), with less of gasoline and low molecular-weight compounds. Table 1 provides a summarized selectivity analysis of other catalysts.

**Table 1:** FTS reaction conditions of  $H_2$ :CO ratio = 2.0, pressure 2.0 MPa.

Catalyst	Particle Size (nm)	Temperature (°C)	Fuel Product Fractions (F)			Data Source (Ref.)
			Gasoline ( $F_G$ )	Diesel + Waxes ( $F_{D+W}$ )	$(F_{D+W})/(F_G)$	
Co/C	11.0	220	29.8	65.7	2.2	[31]
Fe/C	11.3	220	25.6	69.0	2.7	[30]
Fe-Nano Cat <sup>®</sup>	21.1	220	62.2	31.6	0.5	[30]
80%Co-20%Fe/C	8.9	260	19.1	67.2	3.5	[32]
30%Co-70%Fe/C	9.1	260	29.0	55.0	1.9	[32]
Co/C	11.0	260	8.6	23.8	2.8	[32]
Fe/C	11.3	260	19.4	63.9	3.3	[32]
50%Co-50%Fe/C	14.4	260	48.9	32.1	0.7	[32]



Currently, there is a growing interest in understanding the dependency of FTS activity and selectivity on catalyst particle size, but the origin of the particle size effect in FTS remains controversial because of the complexity of the reaction's kinetics and mechanisms [48]. This is in addition to the limitations of in situ characterization set-ups, which can hardly operate at both high temperature and high pressure while simultaneously allowing for real time analysis of the FTS products. From Table 1, it can be concluded that:

- (a). Our high mean particle size catalysts (e.g. 14 or 21 nm) produced more gasoline, with the ratio of the heavy molecules to the light ones,  $(F_{D+W})/(F_C)$  being lower than 1.
- (b). Our lower mean particle size catalysts (~10nm) produced more longer-chain hydrocarbons and the ratio  $(F_{D+W})/(F_C)$  was about 2 and above, regardless of the catalyst composition.

The above results seem to confirm the idea that FTS is a "structure sensitive" reaction since other studies have indicated that within a size range of 3-10nm, a catalyst (Fe/SBA-15) with

higher crystal size presented higher conversion, higher chain growth and lower  $\text{CH}_4$  production [49]. In addition, selectivity also has been seen to be considerably dependent on the metal particle size in Co-based FTS catalysts, and the smaller the particle, the higher the probability of producing longer-chain hydrocarbons [47]. However, the literature reports that smaller Co particles (typically <7 nm) show low turnover frequency that is attributed to stronger CO adsorption [50]. Other authors concur that metal nanoparticles smaller than 6nm lead to both poor activity and inferior selectivity towards the  $\text{C}_{5+}$  fractions [43]. These studies bring to the fore the significant role nanometric materials will play in the future of FTS catalysis. Although some authors have observed that Co particularly remains in the metallic state under FTS conditions [51], often the catalyst composition changes with TOS, but our plasma-synthesized samples have not shown any sign of degradation so far. This conclusion is drawn from the comparative analysis of the fresh and used catalysts by TEM imaging where there was hardly any change in the particle size distribution [30], and from XRD analysis, see Figure 9 [32].

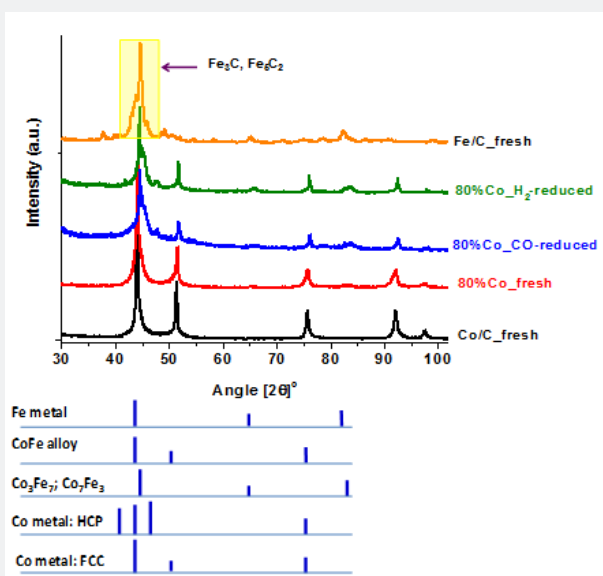


**Figure 9** : Sample XRD patterns of the fresh Co/C, Fe/C and 80%Co-20%Fe/C catalysts compared to the used 80%Co-20%Fe/C after FTS using either  $\text{H}_2$  or CO reduction

The effect of pre-treatment medium was also investigated: depending on catalyst composition, the CO-reduced catalysts showed enhanced selectivity for diesel fraction (50-67%) than catalysts reduced in  $\text{H}_2$  (45-55%) [32]. In addition, it was observed that catalysts containing high concentration of Co as well as those reduced in  $\text{H}_2$  generated more  $\text{H}_2\text{O}$  than those reduced in CO. Further, the presence of Au (that is, in Ni-Co-Fe/C) not only lowered the activity of the Ni-Co-Fe/C catalyst, but it also lowered its capacity to form  $\text{H}_2\text{O}$ , although it had no significant impact on the catalyst's hydrocarbon selectivity [52]. Therefore, the ternary systems were found to be better at  $\text{H}_2$  utilization since they incorporated most of the  $\text{H}_2$  to produce

hydrocarbons rather than forming FTS by-products such as  $\text{H}_2\text{O}$ , and the Mo-Co-Fe/C catalyst being the best at  $\text{H}_2$  utilization efficiency [33].

Enriching the catalyst-surface acidity by Mo-promotion of the Co-Fe/C bimetallic sample improved selectivity for both gasoline fraction (from 19 to 33%) and the overall fuel  $\text{C}_5\text{-C}_{20}$  fraction (from 74 to 87%). This lowered  $\text{H}_2\text{O}$  production by 30%, although at lower CO conversion (~38%). Moreover, Ni-addition to the Co-Fe/C bimetallic sample enhanced catalyst activity from ~42 to 50% CO conversion, and boosted selectivity towards gasoline fraction ( $\text{C}_5\text{-C}_{12}$ ) from ~19 to 50%. The catalysts'  $\alpha$ -values were ~0.8 in the  $\text{C}_{10+}$  region, and from mass

balance, their estimated  $H_2$  efficiency decreased in the order of Mo-Co-Fe/C >> Co-Fe/C > Ni-Co-Fe/C. A summary of the plots is provided in Figure 10. Overall, the Co-Fe bimetallics and the

acidified Co-Fe catalyst (i.e. Mo-Co-Fe/C) were more selective towards diesel formation (~55%) [53].

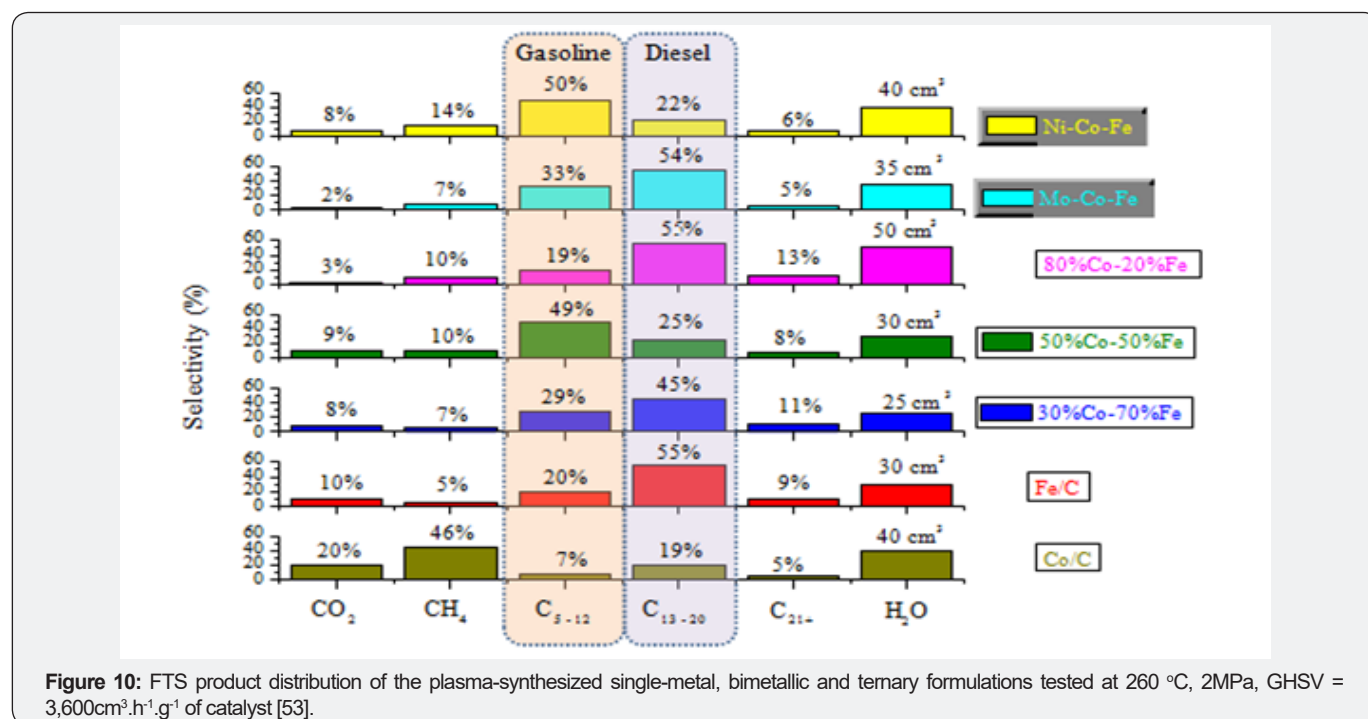


**Figure 10:** FTS product distribution of the plasma-synthesized single-metal, bimetallic and ternary formulations tested at 260 °C, 2MPa, GHSV = 3,600cm<sup>3</sup>.h<sup>-1</sup>.g<sup>-1</sup> of catalyst [53].

## Conclusion

Plasma technology presents a relatively new approach in catalyst synthesis, and when fully developed, it will offer new processing routes with higher overall efficiency in commercial materials processing. Its potential has already been demonstrated in both thermal and non-thermal plasma applications, and it might play a central role in the commercial production of synthetic fuels through Fischer-Tropsch catalysis. Being a single-step process, SPS technology opens prospects for higher energy-efficient, more productive, and environmentally greener processes. In our study, nanometric C-supported catalysts based on Co and Fe with various metal formulations were synthesized through high temperature plasma. The active catalytic species of the metals and the C-matrix support composing both graphitic (G) and amorphous (D; disordered) carbon were all simultaneously generated in situ within the plasma.

With our differently selected chemical compositions, all the catalysts synthesized were tested and found to be highly active for FTS under various reaction conditions. For example, the Co/C catalyst being the most active, indicated ~40% CO conversion at 220 °C, 2MPa pressure, and GHSV = 3,600cm<sup>3</sup>.h<sup>-1</sup>.g<sup>-1</sup> of catalyst. The catalyst showed high selectivity towards the longer hydrocarbon chains with 30% gasoline (C<sub>5</sub>-C<sub>12</sub>), 45% diesel (C<sub>13</sub>-C<sub>20</sub>), and 21% waxes (C<sub>21+</sub>), less than 4% CH<sub>4</sub> and trace amounts of CO<sub>2</sub>. Other catalysts tested include Fe/C, bimetallic Co-Fe/C formulations and those promoted with Ni, Mo, and Au-

Ni. It is currently thought that among other factors that influence FTS when using plasma-synthesized catalysts, particle size takes precedence regardless of composition. This is because those catalysts with smaller particles (mean size range of 9-11nm) were more selective towards the formation of diesel fraction and waxes than those with larger particles of mean size of 14-21nm that produce more gasoline.

## Acknowledgements

We thank the Bio Fuel Net National Center of Excellence -Canada and the National Science & Engineering Research Council of Canada for financial support; Dr. Kossi Béré for technical support on the Plasma reactor system; Henri Gauvin and Jacques Gagné for technical support on the Fischer-Tropsch reactor system; the CCM (Centre de Caractérisation des Matériaux, Université de Sherbrooke) staff for facilitating the characterization: Irène Kelsey Lévesque and Carl St.-Louis for BET surface area analysis, Charles Bertrand for Microscopy (SEM & TEM), and Stéphane Gutierrez for XRD analysis.

## References

1. Dry ME (2002) The Fischer-Tropsch process: 1950–2000. *Catal Today* 71(3-4): 227-241.
2. Dry ME (1990) Fischer-Tropsch synthesis over iron catalysts. *Catal Lett* 7(1-4): 241-252.
3. Khodakov AY, Chu W, Fongarland P (2007) Advances in the development of novel cobalt Fischer-Tropsch catalysts for synthesis of long-chain hydrocarbons and clean fuels. *Chem Rev* 107(5): 1692-1744.

4. Fechete I, Wang Y, Védrine JC (2012) The past, present and future of heterogeneous catalysis. *Catal Today* 189(1): 2-27.
5. Schulz H (1999) Short history and present trends of Fischer-Tropsch synthesis. *Appl Catal A* 186(1-2): 3-12.
6. Mawhood RK, Gazis E, Hoefnagels R, Jong SD, Slade R, et al. (2015) Technological and commercial maturity of aviation biofuels: Emerging options to produce jet from lignocellulosic biomass. Paper presented at the 14<sup>th</sup> International Conference on Sustainable Energy Technologies - SET 2015 (25<sup>th</sup> - 27<sup>th</sup> of August 2015), Nottingham, UK.
7. Chew TL, Bhatia S (2008) Catalytic processes towards the production of biofuels in a palm oil and oil palm biomass-based biorefinery. *Bioresour Technol* 99(17): 7911-7922.
8. Jahangiri H, Bennett J, Mahjoubi P, Wilson K, Gu S, et al. (2014) A review of advanced catalyst development for Fischer-Tropsch synthesis of hydrocarbons from biomass derived syn-gas. *Catal Sci Technol* 4(8): 2210-2229.
9. Klerk DA, Furimsky E (2011) Catalysis in the Refining of Fischer-Tropsch Syncrude. *Platin Met Rev* 55(4): 263-267.
10. Dalai AK, Bakhshi NN, Esmail MN (1992) Characterization studies of plasma-sprayed cobalt and iron catalysts. *Ind Eng Chem Res* 31(6): 1449-1457.
11. Bengoa JF, Alvarez AM, Cagnoli MV, Gallegos NG, Marchetti SG, et al. (2007) Influence of intermediate iron reduced species in Fischer-Tropsch synthesis using Fe/C catalysts. *Appl Catal A* 325(1): 68-75.
12. Ding M, Yang Y, Wu B, Xu J, Zhang C, et al. (2009) Study of phase transformation and catalytic performance on precipitated iron-based catalyst for Fischer-Tropsch synthesis. *J Mol Catal A: Chem* 303(1-2): 65-71.
13. Blanchard J, Abatzoglou N, Eslahpazir-Esfandabadi R, Gitzhofer F (2010) Fischer-Tropsch synthesis in a slurry reactor using a nano-iron carbide catalyst produced by a plasma spray technique. *Ind Eng Chem Res* 49(15): 6948-6955.
14. Chu W, Wang LN, Chernavskii PA, Khodakov AY (2008) Glow-discharge plasma-assisted design of cobalt catalysts for Fischer-Tropsch synthesis. *Angew Chem Int Ed* 47(27): 5052-5055.
15. Jacobs G, Ma W, Gao P, Todic B, Bhatelia T, et al. (2013) The application of synchrotron methods in characterizing iron and cobalt Fischer-Tropsch synthesis catalysts. *Catal Today* 214: 100-139.
16. Hong J, Chu W, Chernavskii PA, Khodakov AY (2010) Cobalt species and cobalt-support interaction in glow discharge plasma-assisted Fischer-Tropsch catalysts. *J Catal* 273(1): 9-17.
17. Govender BB, Iwarere SA, Ramjugernath D (2017) The application of non-thermal plasma catalysis in Fischer-Tropsch Synthesis at very high pressure: The effect of cobalt loading. Paper presented at the World Congress on Engineering and Computer Science (WCECS 2017), San Francisco, USA.
18. Durme VJ, Dewulf J, Leys C, Langenhove VH (2008) Combining non-thermal plasma with heterogeneous catalysis in waste gas treatment: A review. *Appl Catal B* 78(3-4): 324-333.
19. Al-Harrasi WSS, Zhang K, Akay G (2013) Process intensification in gas-to-liquid reactions: plasma promoted Fischer-Tropsch synthesis for hydrocarbons at low temperatures and ambient pressure. *Green Process Synth* 2(5): 479-490.
20. Taghvaei H, Heravi M, Rahimpour MR (2017) Synthesis of supported nanocatalysts via novel non-thermal plasma methods and its application in catalytic processes. *Plasma Process Polym* 14(6): 1-20.
21. Davis BH (2007) Fischer-Tropsch synthesis: comparison of performances of iron and cobalt catalysts. *Ind Eng Chem Res* 46(26): 8938-8945.
22. Aluha J, Bere K, Abatzoglou N, Gitzhofer F (2016) Synthesis of nano-catalysts by induction Suspension Plasma Technology (SPS) for Fischer-Tropsch reaction. *Plasma Chem Plasma Process* 36(5): 1325-1348.
23. Voss M, Borgmann D, Wedler G (2002) Characterization of alumina, silica, and titania supported cobalt catalysts. *J Catal* 212(1): 10-21.
24. Riedel T, Schaub G (2003) Low-temperature Fischer-Tropsch synthesis on cobalt catalysts - effects of CO<sub>2</sub>. *Top Catal* 26(1-4): 145-156.
25. Aluha J, Boahene P, Dalai A, Hu Y, Bere K, et al. (2015) Synthesis and characterisation of nanometric Co/C and Fe/C catalysts for Fischer-Tropsch synthesis: A comparative study using a fixed-bed reactor. *Ind Eng Chem Res* 54(43): 10661-10674.
26. Rutkovskii AE, Vishnyakov LR, Chekhovskii AA, Kirkun NI (2000) Use of plasma technology in creating catalysts on carriers. *Powder Metall Met C+* 39(3-4): 207-209.
27. Liu CJ, Vissokov GP, Jang BWL (2002) Catalyst preparation using plasma technologies. *Catal Today* 72(3-4): 173-184.
28. Aluha-Lulizi J (2017) Low-temperature Fischer-Tropsch synthesis for production of synthetic fuels using nanometric carbon-supported iron and cobalt catalysts, PhD Thesis. Université de Sherbrooke, Sherbrooke (QC), Canada, pp. 281.
29. Blanchard J, Abatzoglou N, Eslahpazir-Esfandabadi R, Gitzhofer F (2010) Fischer-Tropsch synthesis in a slurry reactor using a nano-iron carbide catalyst produced by a plasma spray technique. *Ind Eng Chem Res* 49(15): 6948-6955.
30. Aluha J, Braidy N, Dalai A, Abatzoglou N (2016) Low-temperature Fischer-Tropsch synthesis using plasma-synthesised nanometric Co/C and Fe/C catalysts. *Can J Chem Eng* 94(8): 1504-1515.
31. Aluha J, Hu Y, Abatzoglou N (2017) Effect of CO concentration on the  $\alpha$ -value of plasma-synthesized Co/C catalyst in Fischer-Tropsch synthesis. *Catalysts* 7(2): 1-69.
32. Aluha J, Abatzoglou N (2016) Synthetic fuels from 3- $\phi$  Fischer-Tropsch synthesis using syngas feed and novel nanometric catalysts synthesised by plasma. *Biomass Bioenerg* 95(1): 330-339.
33. Aluha J, Abatzoglou N (2017) Promotional effect of Mo and Ni in plasma-synthesized Co-Fe/C bimetallic nano-catalysts for Fischer-Tropsch synthesis. *J Ind Eng Chem* 50: 199-212.
34. Boulos M, Pfender E (1996) Materials processing with thermal plasmas. *MRS Bull* 21(8): 65-68.
35. Moodley DJ, Loosdrecht VDJ, Saib AM, and Niemantsverdriet HJW (2010) The formation and influence of carbon on cobalt-based Fischer-Tropsch synthesis catalysts: An integrated review. In: Davis BH, Occelli ML (eds.) *Advances in Fischer Tropsch synthesis, catalysts and catalysis*. CRC Press, USA, pp. 49-81.
36. Duvenhage DJ, Coville NJ (1997) Fe: Co/TiO<sub>2</sub> bimetallic catalysts for the Fischer-Tropsch reaction I. Characterization and reactor studies. *Appl Catal A* 153: 43-67.
37. Calderone VR, Shiju NR, Ferré DC, Rothenberg G (2011) Bimetallic catalysts for the Fischer-Tropsch reaction. *Green Chem* 13(8):1950-1959.
38. Tavasoli A, Trépanier M, Abbaslou RMM, Dalai AK, Abatzoglou N, et al. (2009) Fischer-Tropsch synthesis on mono- and bimetallic Co and Fe catalysts supported on carbon nanotubes. *Fuel Process Technol* 90(12):1486-1494.
39. Ishihara T, Horiuchi N, Inoue T, Eguchi K, Takita Y, et al. (1992) Effect of alloying on CO hydrogenation activity over SiO<sub>2</sub>-supported Co-Ni alloy catalysts. *J Catal* 136(1): 232-241.
40. Li S, O'Brien RJ, Meitzner GD, Hamdeh H, Davis BH, et al. (2001) Structural analysis of un promoted Fe-based Fischer-Tropsch catalysts using X-ray absorption spectroscopy. *Appl Catal A* 219(1-2): 215-222.

41. Huyser J, Vuuren VMJ, Kupi G (2010) Advances in Fischer-Tropsch Synthesis, Catalysts, and Catalysis. In: Davis BH, Ocelli ML (eds) The value of a two alpha model in the elucidation of a full product spectrum for Fe-LTFT, pp. 185-198.
42. Herranz T, Rojas S, Pérez-Alonso FJ, Ojeda M, Terreros P, et al. (2006) Genesis of iron carbides and their role in the synthesis of hydrocarbons from synthesis gas. *J Catal* 243(1):199-211.
43. Bezemer GL, Bitter JH, Kuipers HPCE, Oosterbeek H, Holewijn JE, et al. (2006) Cobalt particle size effects in the Fischer-Tropsch reaction studied with carbon nanofiber supported catalysts. *J Am Chem Soc* 128(12): 3956-3964.
44. Wang C, Xu L, Wang Q (2003) Review of directly producing light olefins via CO hydrogenation. *J Nat Gas Chem* 12(1): 10-16.
45. Laan VDGP, Beenackers AACM (1999) Hydrocarbon selectivity model for the gas-solid Fischer-Tropsch synthesis on precipitated iron catalysts. *Ind Eng Chem Res* 38(4): 1277-1290.
46. Dry ME (1982) Catalytic aspects of industrial Fischer-Tropsch synthesis. *J Mol Catal* 17(2-3):133-144.
47. Khassin AA, Yurieva TM, Parmon VN (1998) Fischer-Tropsch synthesis over cobalt-containing unsupported catalysts in slurry reactor: Effect of the metallic Co particle size on the catalyst selectivity. *React Kinet Catal Lett* 64(1): 55-62.
48. Liu JX, Wang P, Xu W, Hensen EJM (2017) Particle size and crystal phase effects in Fischer-Tropsch catalysts. *Engineering* 3(4): 467-476.
49. Cano LA, Cagnoli MV, Fellenz NA, Bengoa JF, Gallegos NG, et al. (2010) Fischer-Tropsch synthesis. Influence of the crystal size of iron active species on the activity and selectivity. *Appl Catal A* 379(1-2): 105-110.
50. Breejen DJP, Radstake PB, Bezemer GL, Bitter JH, Frøseth V, et al. (2009) on the origin of the cobalt particle size effects in Fischer-Tropsch catalysis. *J Am Chem Soc* 131(20): 7197-7203.
51. Ernst B, Libs S, Chaumette P, Kiennemann A (1999) Preparation and characterization of Fischer-Tropsch active Co/SiO<sub>2</sub> catalysts. *Appl Catal A* 186(1-2): 145-168.
52. Aluha J, Abatzoglou N (2017) Gold-promoted plasma-synthesized Ni-Co-Fe/C catalyst for Fischer-Tropsch synthesis. *Gold Bull* 50(2):147-162.
53. Aluha J, Abatzoglou N, Gitzhofer F (2017) Plasma-synthesized carbon-supported nano-catalysts for Fischer-Tropsch synthesis. Conference Paper. The 23<sup>rd</sup> International Symposium on Plasma Chemistry (ISPC 23), Montreal, (QC), Canada.



This work is licensed under Creative Commons Attribution 4.0 License  
DOI: [10.19080/RAPSCI.2018.05.555657](https://doi.org/10.19080/RAPSCI.2018.05.555657)

### Your next submission with Juniper Publishers will reach you the below assets

- Quality Editorial service
- Swift Peer Review
- Reprints availability
- E-prints Service
- Manuscript Podcast for convenient understanding
- Global attainment for your research
- Manuscript accessibility in different formats  
( Pdf, E-pub, Full Text, Audio)
- Unceasing customer service

Track the below URL for one-step submission  
<https://juniperpublishers.com/online-submission.php>